Comparison of turbulent flame speeds from complete averaging and the G-equation

Pedro F. EmbidAndrew J. MajdaPanagiotis E. Souganidis

Citation: **7**, 2052 (1995); doi: 10.1063/1.868452
View online: http://dx.doi.org/10.1063/1.868452
View Table of Contents: http://aip.scitation.org/toc/phf/7/8
Published by the American Institute of Physics

Comparison of turbulent flame speeds from complete averaging and the G-equation

Pedro F. Embid
Program in Applied and Computational Mathematics, Princeton University, Princeton, New Jersey 08544 and Mathematics Department, The University of New Mexico, Albuquerque, New Mexico 87131

Andrew J. Majda
Department of Mathematics and Program in Applied and Computational Mathematics, Princeton University, Princeton, New Jersey 08544

Panagiotis E. Souganidis
Department of Mathematics, University of Wisconsin–Madison, Madison, Wisconsin 53706

(Received 3 February 1995; accepted 3 April 1995)

A popular contemporary approach in predicting enhanced flame speeds in premixed turbulent combustion involves averaging or closure theories for the G-equation involving both large-scale flows and small-scale turbulence. The G-equation is a Hamilton–Jacobi equation involving advection by an incompressible velocity field and nonlinear dependence on the laminar flame speed; this G-equation has been derived from the complete Navier–Stokes equations under the tacit assumptions that the velocity field varies on only the integral scale and that the ratio of the flame thickness to this integral scale is small. Thus there is a potential source of error in using the averaged G-equation with turbulent velocities varying on length scales smaller than the integral scale in predicting enhanced flame speeds. Here these issues are discussed in the simplest context involving velocity fields varying on two scales where a complete theory of nonlinear averaging for predicting enhanced flame speeds without any *ad hoc* approximations has been developed recently by the authors. The predictions for enhanced flame speeds of this complete averaging theory versus the averaging approach utilizing the G-equation are compared here in the simplest context involving a constant mean flow and a small-scale steady periodic flow where both theories can be solved exactly through analytical formulas. The results of this comparison are summarized briefly as follows: The predictions of enhanced flame speeds through the averaged G-equation always underestimate those computed by complete averaging. Nevertheless, when the transverse component of the mean flow relative to the shear is less than one in magnitude, the agreement between the two approaches is excellent. However, when the transverse component of the mean flow relative to the shear exceeds one in magnitude, the predictions of the enhanced flame speed by the averaged G-equation significantly underestimate those computed through complete nonlinear averaging, and in some cases, by more than an order of magnitude. © *1995 American Institute of Physics.*

I. INTRODUCTION

An important area of active research in premixed turbulent combustion involves the accurate prediction of enhanced flame speeds which occur experimentally[1,2] with turbulent velocity fields having several spatiotemporal scales. A popular contemporary approach[3–8] involves nonlinear averaging of the G-equation which is given by

$$G_t + \mathbf{V}\cdot\nabla G = S_L|\nabla G|. \tag{1}$$

In (1), the quantity S_D is the laminar flame speed and $\mathbf{V}(\mathbf{x},t)$ is an incompressible velocity field, i.e., div $\mathbf{V}=0$, while the flame front is given by the level set where G vanishes, i.e., $G=0$ defines the flame front.

The Hamilton–Jacobi equation in (1) emerges from the simplest asymptotic theories[9–11] which exploit the great disparity between the integral length scale of the velocity field, L, and the flame thickness, l_F, through the small parameter $\epsilon = l_F/L \ll 1$ under the assumptions of weak heat release so that thermal expansion effects are ignored and a value of one for the Lewis number; thus, the tacit assumption in the derivation of (1) from the reactive Navier–Stokes equations is that the velocity field, $\mathbf{V}(\mathbf{x},t)$, varies only on the integral scale. Despite this fact, the equation in (1) has been used with velocity fields $\mathbf{V}(\mathbf{x},t)$ involving several length scales much smaller than the integral scale with a variety of averaging and closure procedures regarding the small scales.[4–8] In the present authors' opinion there is a logical flaw, as pointed out above, in using the G-equation from (1) with velocity fields varying on scales smaller than the integral scale and then averaging out these scales to predict enhanced turbulent flame speeds—there is an implied ordering for two small-scale limiting procedures which may not be valid and can affect accurate predictions of turbulent flame speeds.

The main purpose of this paper is to discuss this issue in an unambiguous fashion involving the simplest context with velocity fields which vary on only two scales, both larger than the flame thickness, and with unambiguous exact solutions. Recently two of the authors[12] have developed a mathematically rigorous theory for complete nonlinear averaging without any *ad hoc* approximations of the turbulent reaction diffusion equations which are valid when thermal expansion effects are ignored and the Lewis number is set equal to one. An explicit example of this theory has been developed in detail recently[13] in the simplest context where the large-scale

 1070-6631/95/7(8)/2052/9/$6.00

flow is a constant and the small-scale flow is a steady periodic shear flow. Even this simplest example of the theory displays many qualitative features of turbulent combustion experiments including the "bending" effect where the dependence of the enhanced flame speed on the turbulence intensity is always nonlinear, as well as subtle behavior of the enhanced flame speed on turbulence intensity in the weak turbulence regime depending on the magnitude and direction of the mean flow relative to the shear. A brief summary of this theory involving complete nonlinear averaging is presented in Sec. II.

In this paper, we compare the approach through averaging the G-equation with the complete theory for nonlinear averaging[12,13] described in the previous paragraph for the simple two scale velocity fields given by

$$\mathbf{V}=\bar{\lambda}\bar{\mathbf{u}}+\lambda(v(x_2/\epsilon^{\alpha}),0), \tag{2}$$

where $\bar{\mathbf{u}}=(\cos\bar{\theta},\sin\bar{\theta})$ and $v(y_2)$ is a one-periodic function with unit amplitude representing a small-scale shear flow aligned with the y_1 axis. In (2), $\bar{\lambda}$ is the mean flow intensity, λ is the turbulent intensity, and $\bar{\theta}$ represents the angle between the mean flow and the shear. If we recall from our earlier discussion that $\epsilon=l_F/L\ll 1$ represents the ratio of the flame thickness to the integral scale, the use of the scale, $\mathbf{x}/\epsilon^{\alpha}$, with $0<\alpha<1$, in (1) allows us to include velocity fluctuations on a second scale which is much larger than the flame thickness and much smaller than the integral scale for $\epsilon\ll 1$. In Sec. III, for these simple flows in (2), we calculate exact formulas for the enhanced flame speed predicted from averaging the Hamilton–Jacobi equation in (1). Section IV contains the main results of this paper where for the special flows in (2) the exact formulas for enhanced flame speeds predicted through the averaged G-equation are compared with the exact formulas[13] involving complete nonlinear averaging of the reaction diffusion equations.[12,13] The results of these comparisons are summarized briefly as follows: For all values of the flow field parameters, the enhanced flame speed predicted from the averaged G-equation always underestimates the enhanced flame speed computed through full nonlinear averaging. Whether there is a significant error in utilizing the averaged G-equation compared with complete nonlinear averaging depends on the transverse magnitude of the mean flow, $|\bar{\lambda}\sin\bar{\theta}|$. For $|\bar{\lambda}\sin\bar{\theta}|<1$, there is excellent agreement between the two different averaging approaches for a wide range of turbulent intensities. On the other hand, for $|\bar{\lambda}\sin\bar{\theta}|>1$, the enhanced flame speed from complete nonlinear averaging exceeds the enhanced flame speed predicted by the averaged G-equation significantly and by factors larger than an order of magnitude for a wide range of turbulent intensities.

II. SUMMARY OF THE COMPLETE NONLINEAR AVERAGING THEORY

A. Effective large-scale front equations

Under the physical assumptions of weak heat release and Lewis number equal to one discussed earlier, the propagation of the flame front is given by a single reaction–diffusion advection equation for the temperature field

$$\begin{aligned} &T_t+\mathbf{V}\cdot\nabla T=\epsilon\kappa\Delta T+\epsilon^{-1}f(T), \quad \mathbf{x}\in R^n, \quad 0<t<\infty,\\ &T(\mathbf{x},0)=T_0(\mathbf{x}), \quad \mathbf{x}\in R^n, \end{aligned} \tag{3}$$

where (3) is nondimensionalized in units of the integral scale, with the flame thickness of order $\epsilon=l_F/L\ll 1$, weak diffusion of order ϵ and fast reaction of order ϵ^{-1}. The initial data T_0 is bounded, $0\leqslant T_0\leqslant 1$, with $T=0$ representing the unburnt temperature and $T=1$ the burnt temperature. The support of T_0 is Ω_0.

The nonlinear averaging theory of Majda and Souganidis[12] provides the evolution of the effective flame front in (3) in the limit when $\epsilon\to 0$, and when the incompressible velocity field $\mathbf{V}$ depends on two separated scales,

$$\mathbf{V}=\bar{\mathbf{v}}(\mathbf{x},t)+\lambda\mathbf{v}(\mathbf{x}/\epsilon^{\alpha},t/\epsilon^{\alpha}), \tag{4}$$

with $0<\alpha<1$, so that $\mathbf{V}$ has two components, a mean varying on the integral scale, and a velocity fluctuation involving the turbulent scale, $(\mathbf{x}/\epsilon^{\alpha},t/\epsilon^{\alpha})$, intermediate between the flame thickness and the integral scale. The small scale velocity field $\mathbf{v}$ is assumed to be one-periodic and of unit amplitude, while λ is the ratio of the fluctuation amplitude to the laminar flame speed S_L, and in this model represents the turbulent intensity. The theory also assumes a simple reaction term $f(T)$ of the Kolmogorov–Petrovski–Piskunov (KPP) type,[12–14] the prototype being $f(T)=KT(1-T)$, so that the laminar flame speed is $S_L=2(\kappa f'(0))^{1/2}$. With these assumptions and without further approximations, Majda and Souganidis[12] proved rigorously that in the limit $\epsilon\to 0$ the effective equation for the propagation of the flame front is given by the *variational inequality*

$$\begin{aligned} &\max(Z_t-H(\nabla Z,\mathbf{x},t)-f'(0),Z)=0, \quad \mathbf{x}\in R^n, \quad 0<t<\infty,\\ &Z(x,0)=\begin{cases} 0, & \mathbf{x}\in\Omega_0,\\ -\infty, & \mathbf{x}\in R^n\backslash\Omega_0, \end{cases} \end{aligned} \tag{5}$$

where at any time $t>0$ the location of the flame front is given as the boundary of the set $\{\mathbf{x}\in R^n: Z(\mathbf{x},t)<0\}$. The variables T and Z in (3), (5) are related by $T=\exp[\epsilon^{-1}(Z+o(1))]$ as $\epsilon\to 0$.

The nonlinear function $H(\mathbf{p},\mathbf{x},t)$ in the variational inequality (5) is the *effective Hamiltonian*. The function H is obtained as a nonlinear eigenvalue problem via nonlinear averaging over the intermediate turbulent scale: for given $(\mathbf{p},\mathbf{x},t)$, there is a unique $H(\mathbf{p},\mathbf{x},t)$ and $\psi(\mathbf{y},\tau)$ periodic in the period cell $Q\times I=[0,1]^n\times[0,1]$ such that

$$\begin{aligned} &\psi_\tau-\kappa|\mathbf{p}+\nabla_y\psi|^2+(\bar{\mathbf{v}}(\mathbf{x},t)+\lambda\mathbf{v}(\mathbf{y},\tau))\cdot(\mathbf{p}+\nabla_y\psi)\\ &\quad=-H(\mathbf{p},\mathbf{x},t). \end{aligned} \tag{6}$$

An interesting consequence of the variational inequality (5) is that there are velocity fields $\mathbf{V}$ for which the resulting effective flame front does not evolve, according to Huygens principle.[12] This type of situation cannot be accounted for by the G-equation because the evolution of the front in (1) is given by a Hamilton–Jacobi equation. However, in the present paper we confine our attention to velocity fields for which the variational inequality is equivalent to Huygens principle; it is sufficient to consider the subclass of velocity

fields in (4) with $\bar{\mathbf{v}}(\mathbf{x},t)$ a constant.[12] In this case the variational inequality (5) is equivalent to the Hamilton–Jacobi equation[12]

$$u_t = F(\nabla u), \tag{7}$$

where $u(\mathbf{x},t)=0$ describes the front and $F(\mathbf{n})$ represents the *effective flame front velocity* in the normal direction $\mathbf{n}$. Moreover, in this case the effective front speed $F(\mathbf{n})$ in the direction $\mathbf{n}$ is given by minimization along a ray[12]

$$F(\mathbf{n}) = \inf_{r>0}\{[1/4 + H(r\mathbf{n})]/r\}, \tag{8}$$

where $H(\mathbf{p})$ is the effective Hamiltonian given by the cell problem in (6).

B. Explicit exact formulas for simple shear layers

The computation of the effective Hamiltonian H from the cell problem (6) is in general a challenging problem. However, for the simple shear layer velocity fields in (2), explicit analytical formulas for the effective Hamiltonian H have been derived.[12,13] The interested reader can consult Refs. 12 and 13 for the explicit formulas. In Ref. 13 these formulas have been used to study the effective flame front speed F in (8), its anisotropic dependence on the direction $\mathbf{n}=(\cos\theta, \sin\theta)$, and changes with the different flow parameters in (2): the mean flow intensity $\bar{\lambda}$, the mean flow angle $\bar{\theta}$ between the mean flow and shear directions, and the turbulence intensity λ.[13]

Even for the case of the simple shear layer flow (2) the effective flame velocity has a rich and subtle behavior. The dependence of the effective flame speed on the turbulence intensity is nonlinear and displays the bending effect.[13] In the limit of weak turbulence intensity, $\lambda \to 0$, the asymptotic dependence of the effective front velocity F on the turbulence intensity λ changes drastically depending on the magnitude $|\bar{\lambda}\sin\bar{\theta}|$ which represents the ratio of the component of the mean flow orthogonal to the shear divided by the laminar flame speed S_L. When $|\bar{\lambda}\sin\bar{\theta}|<1$ the asymptotic dependence of F on λ is linear but when $|\bar{\lambda}\sin\bar{\theta}|>1$ it shifts to quadratic. Also, changing the form of the small scale shear $v(y_2)$ in (2) shows that the effective flame speed F depends only on the gross features and not on the fine details of the small-scale shear flow. For the specific details the reader can consult Ref. 13.

III. APPROACH VIA NONLINEAR AVERAGING OF THE G-EQUATION

A. Nonlinear averaging of the G-equation

Here we briefly describe the averaging procedure for the G-equation in the context of separated scale velocity fields. This procedure is both mathematically rigorous[12,15,16] and also exactly equivalent to the alternative approach utilized in Ref. 3 involving finding periodic traveling waves. Assume the incompressible velocity $\mathbf{V}$ in (1) is given with two separated spatial scales as in (2), $\mathbf{V}=\bar{\mathbf{v}}(\mathbf{x})+\lambda\mathbf{v}(\mathbf{x}/\epsilon^{\alpha})$. We seek a solution G of (1) given by the asymptotic expansion

$$G = G^0(\mathbf{x},t) + \epsilon^{\alpha}G^1(\mathbf{x},\mathbf{x}/\epsilon^{\alpha},t) + \cdots. \tag{9}$$

Plugging (9) into (1) and collecting the terms of leading order yields

$$G_t^0 + (\bar{\mathbf{v}}(\mathbf{x}) + \lambda\mathbf{v}(\mathbf{y}))\cdot(\nabla_x G^0 + \nabla_y G^1(\mathbf{x},\mathbf{y},t)) - |\nabla_x G^0 + \nabla_y G^1(\mathbf{x},\mathbf{y},t)||_{\mathbf{y}=\mathbf{x}/\epsilon^{\alpha}} = 0. \tag{10}$$

The equation in (10) yields a self-consistent equation involving G^0 alone provided that we can solve the associated nonlinear eigenvalue problem, the cell problem, obtained by nonlinear averaging in the small-scale variable over the period cell: for given $(\mathbf{p}, \mathbf{x})$, there is a unique $U(\mathbf{p},\mathbf{x})$ and a one-periodic solution $\psi(\mathbf{y})$ of the cell problem

$$(\bar{\mathbf{v}}(\mathbf{x}) + \lambda\mathbf{v}(\mathbf{y}))\cdot(\mathbf{p} + \nabla_y\psi) - |\mathbf{p} + \nabla_y\psi| = U(\mathbf{p},\mathbf{x}), \tag{11}$$

where the solution of (11) is understood in the viscosity sense.[12,15,16] With this value of $U(\mathbf{p},\mathbf{x})$ given by (11) substituted back into (10), we obtain the effective equation of nonlinear averaging of the G-equation

$$G_t^0 + U(\nabla_x G^0, \mathbf{x}) = 0. \tag{12}$$

From (11) it is clear that $U(\mathbf{p},\mathbf{x})$ is a homogeneous function of degree one in $\mathbf{p}$. Therefore, the effective flame speed velocity at the point $\mathbf{x}$ and in the direction $\mathbf{n}$ for the averaged G-equation is given by $U(\mathbf{n},\mathbf{x})$.

B. Explicit formulas for the effective flame speed of the averaged G-equation

Next we compute explicit formulas for the effective flame speed $U(\mathbf{n})$, $\mathbf{n}=(\cos\theta,\sin\theta)$, of the averaged G-equation, for the special case where the velocity field $\mathbf{V}$ is given by the simple shear layer (2). Since the small-scale shear layer $v(y_2)$ is a function of only one variable it is enough, by the uniqueness of $U(\mathbf{n})$, to seek a one-periodic solution $\psi(y_2)$ which depends only on the variable y_2, thus reducing the two-dimensional cell problem in (11) to a nonlinear ODE eigenvalue problem of the form (for convenience we remove the subscript in y_2)

$$\mathscr{F}(\psi'(y)) = U + \mathscr{V}(y), \tag{13}$$

where $\psi(y)$ is one-periodic and $\mathscr{F}(\psi)$ and $\mathscr{V}(y)$ are given by

$$\mathscr{F}(\psi) = [(\psi + \sin\theta)^2 + \cos^2\theta]^{1/2} + \bar{\lambda}\sin\bar{\theta}(\psi + \sin\theta), \tag{14}$$

$$\mathscr{V}(y) = -(\bar{\lambda}\cos\bar{\theta} + \lambda v(y))\cos\theta. \tag{15}$$

In order to compute the effective flame speed U from (13) we must invert $\mathscr{F}$ in (13) and average the result over a unit period. However, this approach needs to be modified when $\mathscr{F}$ is not invertible. The function $\mathscr{F}$ in (14) behaves differently depending on whether $|\bar{\lambda}\sin\bar{\theta}|$ is larger or smaller than one. If $|\bar{\lambda}\sin\bar{\theta}|>1$ then $\eta=\mathscr{F}(\psi)$ is invertible with $\mathscr{F}^{-1}$ given by

$$\mathscr{F}^{-1}(\eta) = \{(\bar{\lambda}\sin\bar{\theta})\eta - \mathrm{sign}(\bar{\lambda}\sin\bar{\theta}) \times [\eta^2 + \cos^2\theta((\bar{\lambda}\sin\bar{\theta})^2 - 1)]^{1/2}\} \times [(\bar{\lambda}\sin\bar{\theta})^2 - 1]^{-1} - \sin\theta. \tag{16}$$

On the other hand, when $|\bar{\lambda}\sin\bar{\theta}|<1$ then $\psi=\mathscr{F}(\eta)$ has two branches $\mathscr{F}_{\pm}^{-1}$

$$\mathscr{F}_{\pm}^{-1}(\eta)=\{-(\bar{\lambda}\sin\bar{\theta})\eta\pm[\eta^2-\cos^2\theta(1-(\bar{\lambda}\sin\bar{\theta})^2)]^{1/2}\}[1-(\bar{\lambda}\sin\bar{\theta})^2]^{-1}-\sin\theta. \tag{17}$$

The solution of the cell problem (13) and the formulas for the effective flame speed U are a straightforward generalization of the analysis done in Refs. 12 and 15 for the special case, where $\mathscr{F}(\psi)=\psi^2$ in (13). The result is that for any given direction $\mathbf{n}=(\cos\theta,\sin\theta)$ there is a unique solution $U(\mathbf{n})$ and $\psi(y)$ of the cell problem (13). If $\langle\cdot\rangle$ denotes the average over the period cell, then U is given explicitly as follows:

(1) If $|\bar{\lambda}\sin\bar{\theta}|>1$ then U solves the nonlinear algebraic equation

$$\langle\mathscr{F}^{-1}(U+\mathscr{V}(y))\rangle=0. \tag{18}$$

(2) If $|\bar{\lambda}\sin\bar{\theta}|<1$ define the minimal speed U_* by

$$U_*=\min\mathscr{F}(\psi)-\min\mathscr{V}(y)=(1-(\bar{\lambda}\sin\bar{\theta})^2)^{1/2}|\cos\theta|+\bar{\lambda}\cos\bar{\theta}\cos\theta+\lambda\max(v(y)\cos\theta). \tag{19}$$

It is clear from (13) that U_* satisfies $U_*\leq U$. Now the effective flame speed U is given by one of the following mutually exclusive alternatives where U either assumes the minimal speed U_* or else it is obtained by averaging over one of the branches $\mathscr{F}_{\pm}^{-1}$ in similar fashion as in (18).

(i) If $\langle\mathscr{F}_{-}^{-1}(U_*+\mathscr{V}(y))\rangle\leq 0\leq\langle\mathscr{F}_{+}^{-1}(U_*+\mathscr{V}(y))\rangle$, then U is given by

$$U=U_*. \tag{20}$$

(ii) If $\langle\mathscr{F}_{-}^{-1}(U_*+\mathscr{V}(y))\rangle>0$, then $U>U_*$ solves the equation

$$\langle\mathscr{F}_{-}^{-1}(U+\mathscr{V}(y))\rangle=0. \tag{21}$$

(iii) If $\langle\mathscr{F}_{+}^{-1}(U_*+\mathscr{V}(y))\rangle<0$, then $U>U_*$ solves the equation

$$\langle\mathscr{F}_{+}^{-1}(U+\mathscr{V}(y))\rangle=0. \tag{22}$$

The explicit analytical formulas for U in (18)–(22) are algebraically complex but are readily evaluated numerically using standard quadrature and root finding techniques.

Using these formulas we can study the effective flame velocity U as a function of the direction angle θ. Since we are interested in studying the effects of the small fluctuations of the shear flow on the effective flame speed, it is convenient to study the *enhanced flame velocity* U_e defined by

$$U_e=U-1-\bar{\lambda}\cos(\theta-\bar{\theta}), \tag{23}$$

that is, we subtract from the effective flame velocity U the contribution of the laminar front velocity which ignores the small-scale fluctuations. Next we study the enhanced flame velocity U_e for the representative case where the flow field (2) has the periodic small-scale shear fluctuation given by the simple sine profile $v(y_2)=\sin 2\pi y_2$, and where we fix the mean flow angle in (2) to be $\bar{\theta}=30°$. We study two illustrative cases corresponding to weak transverse mean flow, $|\bar{\lambda}\sin\bar{\theta}|<1$, and strong transverse mean flow, $|\bar{\lambda}\sin\bar{\theta}|>1$.

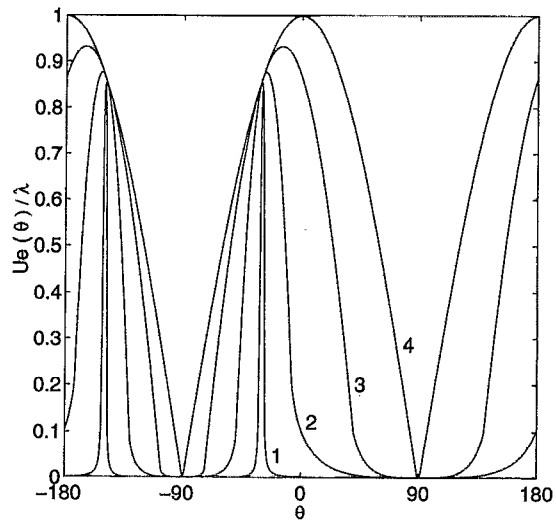

FIG. 1. Plot of the enhanced flame velocity $U_e(\theta)/\lambda$ for the sine shear with mean flow angle $\bar{\theta}=30°$ and mean flow intensity $\bar{\lambda}=1$. The curves 1–4 correspond to increasing turbulent intensity $\lambda=0.001$, 0.1, 1, and 100.

With the chosen value of the mean flow angle, the threshold value of the mean-flow intensity for which $|\bar{\lambda}\sin\bar{\theta}|=1$ is $\bar{\lambda}=2$.

Figure 1 shows the enhanced flame velocity $U_e(\theta)$ for the case of a weak transverse mean flow with mean flow intensity $\bar{\lambda}=1$ and for selected values of the turbulent intensity λ in the range $10^{-3}\leq\lambda\leq 10^2$. Figure 1 clearly displays the anisotropic dependence of the enhanced flame speed on the direction angle θ, where clearly there is no enhancement in the direction orthogonal to the shear, and there are two directions with maximum enhancement symmetrically situated around $\theta=-90°$. Figure 1 also shows that as the turbulent intensity λ increases, the bands of directions, where there is substantial enhancement, grow broader, and that the directions of maximum flame velocity $U_e(\theta)$ shift towards the shear flow direction $\theta=0°$. For fixed λ the directions of maximum enhancement are dependent on the mean flow angle $\bar{\theta}$ and shift towards $\theta=-90°$ as the mean flow angle $\bar{\theta}$ increases towards $\bar{\theta}=90°$. Figure 1 also shows that for a weak transverse mean flow, the dependence of the enhanced flame speed U_e on the turbulence intensity λ is essentially linear for the range considered.

Figure 2 shows the enhanced flame speed $U_e(\theta)$ for a strong transverse mean flow with mean flow intensity $\bar{\lambda}=10$ and for selected values of the turbulence intensity λ in the range $10^{-3}\leq\lambda\leq 10$. Figure 2 again makes evident the anisotropic dependence of $U_e(\theta)$ although the profiles of U_e are different from the weak transverse mean depicted in Fig. 1. In this case, the direction of maximum enhancement is slightly shifted away from the shear direction, and the band of direction angles, where there is substantial enhancement, do not narrow with decreasing turbulence intensity. In fact, it is striking to see how little $U_e(\theta)$ changes over three orders of magnitude in λ, making it clear that for the strong transverse mean case the dependence of the enhanced flame speed on the turbulence intensity is quadratic rather than linear

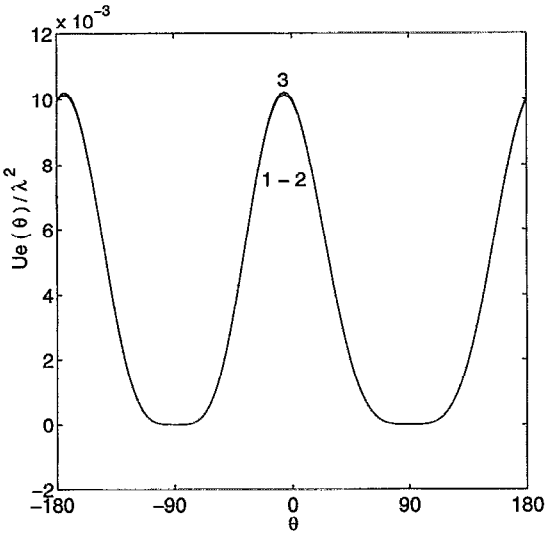

FIG. 2. Plot of the enhanced flame velocity $U_e(\theta)/\lambda^2$ for the sine shear with mean flow angle $\bar{\theta}=30°$ and mean flow intensity $\bar{\lambda}=10$. The curves 1–3 correspond to increasing turbulent intensity $\lambda=0.001$, 0.1, and 1.

over the weak turbulence regime. For strong turbulence, $U_e(\theta)$ resembles the corresponding profiles in Fig. 1 and the dependence on λ also converges to linear. Figures 1 and 2 also show the important effect that the mean flow has on the qualitative behavior of the effective flame speed.

We close this section with the remark that in previous work Ashurst and Sivashinsky[3] studied the effects of a periodic shear flow on the effective flame speed. Their analysis was restricted to the sinusoidal shear layer without a mean flow, and the effective flame speed was computed only for the directions $\theta=0°$ and $\theta=45°$. The present analysis generalizes their work; we compute the effective flame velocity for all the flame front directions and we exhibit its anisotropic nature. More importantly, we include the mean flow with its subtle effects on the effective flame speed. Our formulation of the effective flame front velocity in (18)–(22) allows for arbitrary forms of the small-scale shear $v(y_2)$, for example multimode Fourier shear profiles like the one considered in the next section.

IV. COMPARISON OF THE COMPLETE NONLINEAR AVERAGING THEORY VERSUS THE AVERAGED G-EQUATION

Here we compare the predictions of the complete nonlinear averaging theory from Ref. 13 with the nonlinear averaging of the G-equation from Sec. III for the case where the flow field is of the form in (2). At first sight one finds several qualitative similarities. Both theories predict different behavior for the effective flame speed depending on whether the magnitude of the transverse mean flow, $|\bar{\lambda}\sin\bar{\theta}|$, is larger or smaller than one. The anisotropic dependence of the enhanced flame speed predicted by both theories in the weak and strong transverse mean flow regimes is also qualitatively similar. Both theories predict similar qualitative behavior of the effective flame speed on the turbulence intensity, including the nature of the asymptotic dependence of the effective flame velocity on the turbulence intensity in the limits of weak ($\lambda\to 0$) and strong ($\lambda\to\infty$) turbulence intensity. However, these analogies can be misleading and, as the quantitative comparison of the two theories done below shows, the discrepancies are substantial and subtle. This quantitative comparison shows that the averaged G-equation always predicts slower enhanced flame speeds than the complete nonlinear averaging theory. Interestingly, whether this discrepancy is severe or not depends on the parameter $|\bar{\lambda}\sin\bar{\theta}|$. The discrepancy of the predicted flame speeds in both theories is small when $|\bar{\lambda}\sin\bar{\theta}|<1$ but can be very substantial when $|\bar{\lambda}\sin\bar{\theta}|>1$.

For the purpose of comparison we use representative flow fields in (2) with the small-scale shear fluctuation given by a single Fourier mode $v(y_2)=\sin(2\pi y_2)$, as in Sec. III, or the multiple Fourier mode profile

$$v(y_2)=\cos(2\pi y_2)+(1/2)\sin(2\pi y_2)+(1/2)\cos(4\pi y_2)+(1/2)\cos(6\pi y_2)-(1/4)\sin(6\pi y_2)+(1/2)\cos(8\pi y_2), \tag{24}$$

suitably normalized so that $v(y_2)$ has unit amplitude. The trigonometric polynomial in (24) was considered in Ref. 13 as an example of small-scale shear profile with a complex structure and asymmetrical form. We also fix the value of the mean flow angle to be $\bar{\theta}=30°$, as in Sec. III, so that the threshold value where $|\bar{\lambda}\sin\bar{\theta}|=1$ is given by $\bar{\lambda}=2$. The enhanced flame velocity U_e from nonlinear averaging of the G-equation is defined by (23); the enhanced flame velocity F_e from complete nonlinear averaging is similarly defined, with U replaced by the effective flame velocity F given in (8) by complete nonlinear averaging. Below we investigate the quantitative predictions of both theories of the enhanced flame speed for representative values of the mean flow intensity corresponding to weak and strong transverse mean flows, and compare the predicted maximum enhanced flame speeds over a wide range of turbulent intensities, again for selected representative values of the mean flow intensity.

A. Comparison for weak transverse mean flows ($|\bar{\lambda}\sin\bar{\theta}|<1$)

First, we compare the predicted effective flame front velocities for the case where the small scale shear is a sine profile. Figure 3 shows the values of the enhanced flame speeds F_e predicted by complete nonlinear averaging, U_e predicted by averaging the G-equation, and their difference U_e-F_e, all normalized by the maximum amplitude $\max U_e$ of U_e. We use this normalization by $\max U_e$ throughout the discussion below. The mean flow intensity is $\bar{\lambda}=1$ and the turbulence intensity is $\lambda=0.1$.

Figure 3 shows that the enhanced flame speed U_e obtained from the averaged G-equation underpredicts the value F_e of the enhanced flame speed obtained from complete averaging for all the direction angles. In this case the agreement of the predicted flame speeds is excellent. The largest discrepancies are localized in a narrow band of directions near the orthogonal direction corresponding to $\theta=90°$, where there is very little enhancement of the flame speed anyway.

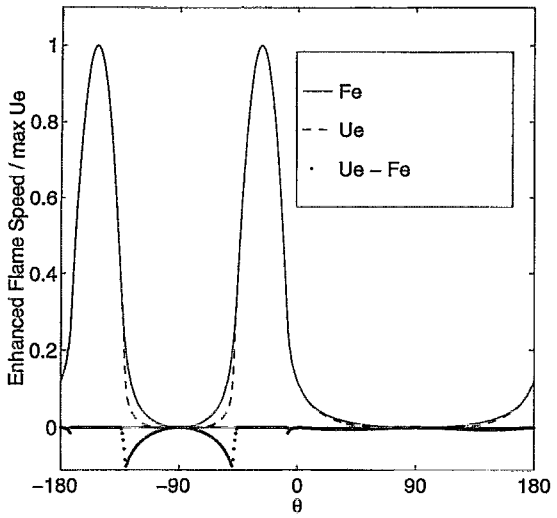

FIG. 3. Plot of the enhanced flame speeds U_e (averaged G-equation), F_e (complete nonlinear averaging), and their difference for sine shear with mean flow intensity $\bar{\lambda}=1$, mean flow angle $\bar{\theta}=30°$, and turbulent intensity $\lambda=0.1$.

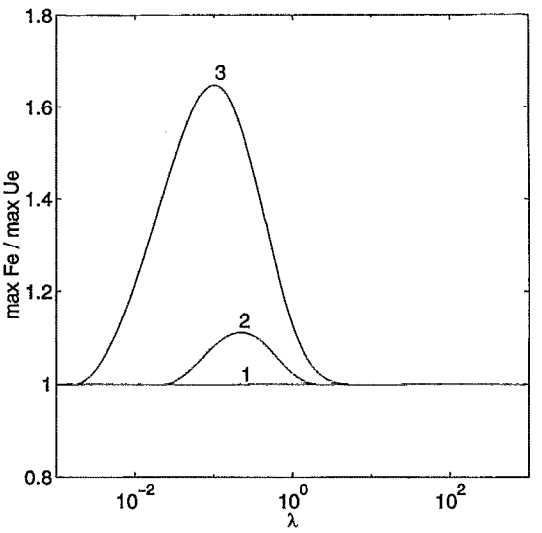

FIG. 5. Semilog plot of max F_e/max U_e for sine shear with mean flow angle $\bar{\theta}=30°$. The curves 1–3 correspond to increasing mean flow intensity $\bar{\lambda}=1.8$, 1.95, and 1.99.

The maximum value of this difference is about 0.1, i.e., about 10% of max U_e. However, in the region where there is substantial enhancement of the flame speed the agreement is excellent with a very small difference max F_e − max U_e $=0.7\times10^{-6}$. Although one may be tempted to think that the predictions of both theories converge in the limit as $\bar{\lambda}\to0$ this is not the case, the discrepancies persist even at $\bar{\lambda}=0$ where the profiles look very similar to those in Fig. 3, and where $\max(F_e-U_e)=0.07$ is even larger.

Figure 4 is a similar plot to that in Fig. 3, with $\lambda=0.1$ but with the mean flow intensity $\bar{\lambda}=1.95$ closer to the threshold value $\bar{\lambda}=2$. In this case the differences between the predictions from both theories are more apparent. Although the qualitative features of both profiles are similar, the averaged G-equation again underpredicts the values of the flame speed. The band of directions where there are substantial differences in the flame speed is still localized, but in contrast with the situation discussed in Fig. 4, this band now extends to the region where there is maximum enhancement. The maximum discrepancy in the velocities is $\max(F_e-U_e)=0.54$, whereas the difference of the maximum predicted flame speeds in both theories for this case is max F_e − max $U_e=0.08$. Although in this case the discrepancies in the predicted flame speeds are larger, they are of the same order of magnitude of max U_e.

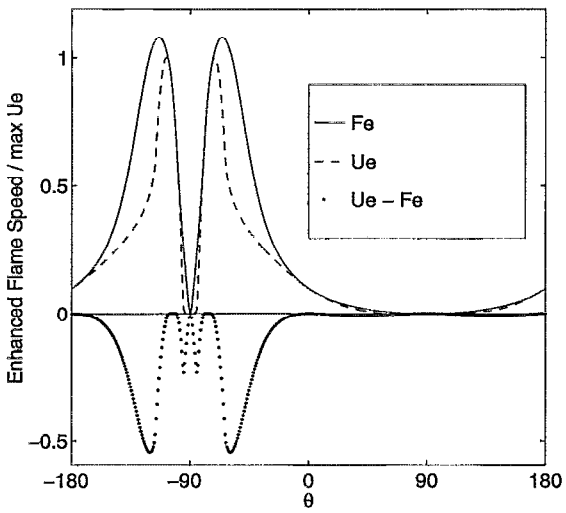

FIG. 4. Plot of the enhanced flame speeds U_e (averaged G-equation), F_e (complete nonlinear averaging), and their difference for sine shear with mean flow intensity $\bar{\lambda}=1.95$, mean flow angle $\bar{\theta}=30°$, and turbulent intensity $\lambda=0.1$.

Figure 5 depicts the ratio of the maximum enhanced flame speed predicted by both theories, max $F_e(\theta)$/max $U_e(\theta)$ as a function of the turbulent intensity λ in the range $10^{-3}\leqslant\lambda\leqslant10^{3}$, for selected values of the mean flow intensity $\bar{\lambda}=1.8$, 1.95, and 1.99, all below the threshold value $\bar{\lambda}=2$. Figure 5 shows that the predicted maximum flame speed in both theories agree very well for values of $\bar{\lambda}$ far enough below the threshold value $\bar{\lambda}=2$. For the values $\bar{\lambda}=1.95$ and 1.99, the difference in the predictions is appreciable but not dramatic, with the maximum ratio of about 1.65 for $\bar{\lambda}=1.99$. Clearly the discrepancy in the maximum flame speed predicted by both theories increases as the mean flow intensity approaches the threshold value $\bar{\lambda}=2$. Figure 5 also shows that the discrepancy in the maximum enhanced flame speeds occurs in the range from low to moderate turbulence intensity, corresponding to $10^{-3}\leqslant\lambda\leqslant10$ for the curves depicted.

B. Comparison for strong transverse mean flow ($|\bar{\lambda}\sin\bar{\theta}|<1$)

When the mean flow intensity $\bar{\lambda}$ crosses above the threshold value $\bar{\lambda}=2$, the discrepancies in the predictions of both theories are more dramatic. In Fig. 6 we compare the

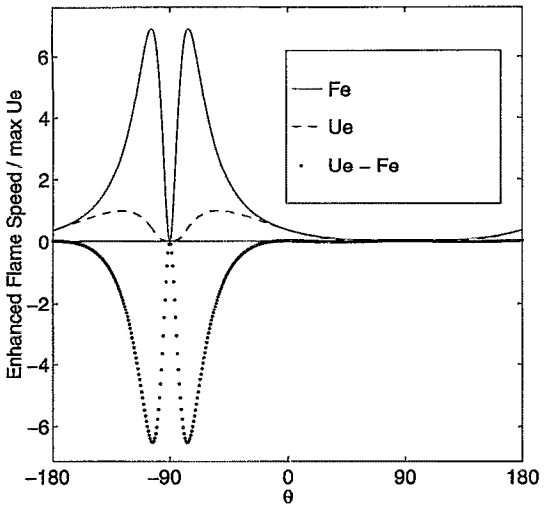

FIG. 6. Plot of the enhanced flame speeds U_e (averaged G-equation), F_e (complete nonlinear averaging), and their difference for sine shear with mean flow intensity $\bar{\lambda}=2.05$, mean flow angle $\bar{\theta}=30°$, and turbulent intensity $\lambda=0.01$.

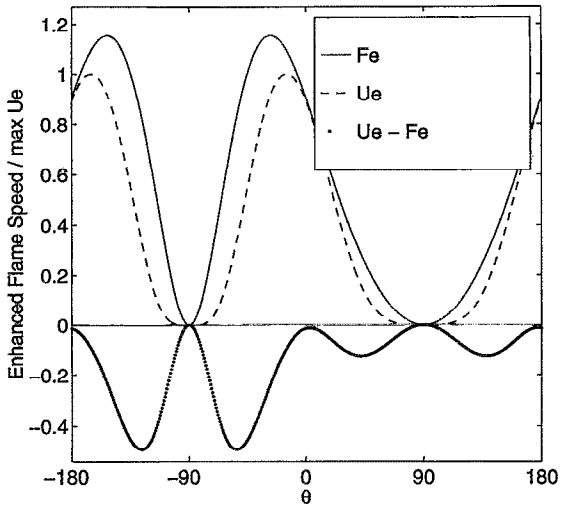

FIG. 7. Plot of the enhanced flame speeds U_e (averaged G-equation), F_e (complete nonlinear averaging), and their difference for sine shear with mean flow intensity $\bar{\lambda}=4$, mean flow angle $\bar{\theta}=30°$, and turbulent intensity $\lambda=1$.

effective flame speeds predicted by both theories in the strong transverse mean regime where we continue to use the simple sine shear layer $v(y_2)=\sin(2\pi y_2)$ for the small-scale fluctuations. The value of the mean flow intensity is $\bar{\lambda}=2.05$, slightly above the threshold value $\bar{\lambda}=2$, and the turbulent intensity is $\lambda=0.01$.

Figure 6 depicts the values of F_e, U_e, and U_e-F_e, normalized by $\max U_e$. Again, we notice that overall the averaged G-equation underpredicts the flame velocity. However, here we observe a severe discrepancy in the predictions of the two theories. The maximum difference of the two speeds is quite large, $\max(F_e-U_e)=6.49$, and even the difference in the predicted maximum is large, $\max F_e-\max U_e=5.92$. By comparing Figs. 4 and 6, we observe that as the mean flow intensity increases above the threshold value of $\bar{\lambda}=2$, the flame speeds predicted by the averaged G-equation can no longer fit the values of the flame speed obtained with complete averaging in the region where the flame speed is largest. Otherwise, the flame speeds depicted in Figs. 4 and 6 are qualitatively similar, both with a localized region where the discrepancy in the predicted flame speeds is appreciable.

Figure 7 depicts, again, the normalized values of F_e, U_e, and U_e-F_e for the case where the mean flow intensity $\bar{\lambda}=4$ is well above the threshold value $\bar{\lambda}=2$, and the turbulence intensity is $\lambda=1$. Figure 7 again shows the flame velocity is underpredicted by the averaged G-equation. In contrast with the cases so far discussed, the directions for which there is a substantial discrepancy in the predictions of both theories are no longer localized. On the other hand, the magnitude of the discrepancy has been reduced considerably when compared with the case $\bar{\lambda}=2.05$ just discussed. Here we have only $\max(F_e-U_e)=0.49$, and for the difference of the predicted maximum flame speeds $\max F_e-\max U_e=0.15$.

Next we study the predictions of the maximum enhanced flame speed given by both theories over a wide range of the turbulence intensity parameter. Figure 8 shows log–log plot of the ratio of the maximum enhanced flame speed predicted by both theories, $\max F_e(\theta)/\max U_e(\theta)$ as a function of the turbulent intensity λ in the range $10^{-3}\leqslant\lambda\leqslant10^{3}$. We used the simple sine profile as small scale shear layer, and the selected values of the mean flow intensity $\bar{\lambda}=2.05$, 2.2, 2.5, 5, and 50, all above the threshold value $\bar{\lambda}=2$.

Figure 8 shows that for values of the mean flow intensity $\bar{\lambda}$ close and above the threshold value $\bar{\lambda}=2$ there can be tremendous discrepancies in the predicted values of the flame speeds as given by both theories. For example, for $\bar{\lambda}=2.01$ the maximum value of the ratio

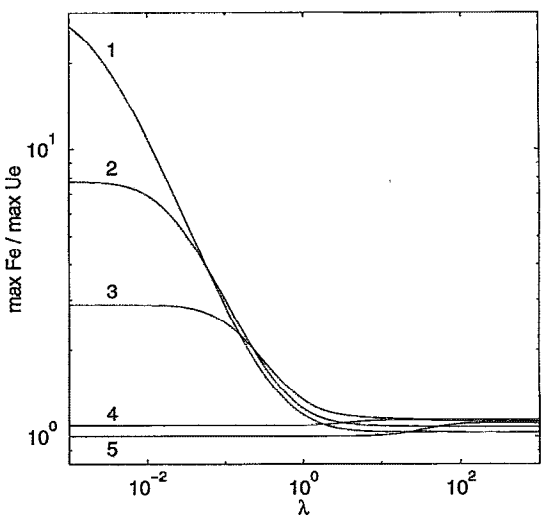

FIG. 8. Log–log plot of $\max F_e/\max U_e$ for sine shear with mean flow angle $\bar{\theta}=30°$. The curves 1–5 correspond to increasing mean flow intensity $\bar{\lambda}=2.01$, 2.05, 2.2, 5, and 50.

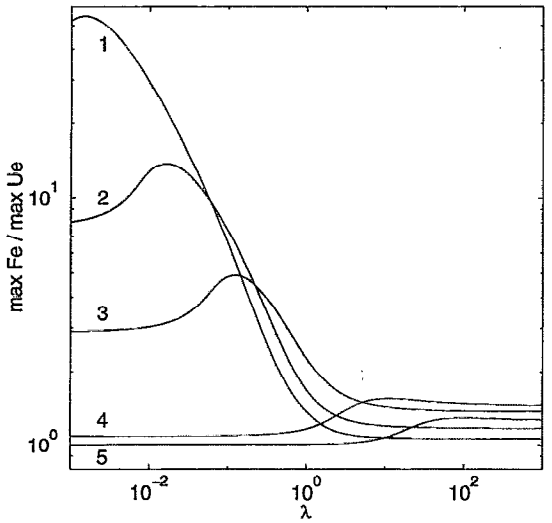

FIG. 9. Log–log plot of max F_e/max U_e for multiple Fourier mode shear with mean flow angle $\bar{\theta}=30°$. The curves 1–5 correspond to increasing mean flow intensity $\bar{\lambda}=2.01$, 2.05, 2.2, 5, and 20.

max F_e/max $U_e=26.8$. For $\bar{\lambda}=2.05$ and 2.2 the corresponding values are still large and equal to 7.7 and 2.9, respectively. Figure 8 clearly shows that for values of the mean flow intensity $\bar{\lambda}$ above $\bar{\lambda}=2$, the maximum enhanced flame speed predicted by complete nonlinear averaging can easily be an order of magnitude larger than the speed predicted by the averaged G-equation over a wide range of the turbulent intensity. Figure 8 shows that for values of $\bar{\lambda}$ close to $\bar{\lambda}=2$, the ratio max F_e/max U_e is large over the low range of turbulent intensity λ and gets close to one for large values of λ. On the other hand, for the higher values of the mean flow intensity $\bar{\lambda}=5$, 50, the situation is reversed and the ratio max F_e/max U_e is maximum at high values of the turbulent intensity, but in this case the values of the maxima are small, about 1.14 for $\bar{\lambda}=5$ and 1.12 for $\bar{\lambda}=50$. Although it is hard to see in Fig. 8, we point out that the curves for $\bar{\lambda}=5$ and 50 are not monotonic.

Finally, Fig. 9 shows a log–log plot of the ratio max F_e/max U_e of the maximum enhanced flame speeds predicted by both theories for the case where the small scale shear in (2) is given by the trigonometric polynomial in (24). The turbulent intensity is again in the range $10^{-3}\leqslant\lambda\leqslant 10^3$ and the selected values of the mean flow intensity are $\bar{\lambda}=2.01$, 2.05, 2.2, 5, and 20, all above the threshold value $\bar{\lambda}=2$.

Figure 9 shows the dramatic effect that the small-scale shear can have in the predictions of the averaged G-equation versus complete averaging, through the asymmetry in the small-scale fluctuations produced by the higher-order modes. For $\bar{\lambda}=2.01$ the maximum value of max F_e/max $U_e=54.8$, so the complete averaged theory predicts maximum enhanced flame speeds more than 50 times larger than those predicted by averaging the G-equation! The values of the maximum ratio for $\bar{\lambda}=2.05$ and 2.2 are 13.7 and 4.89, respectively. In general, all the features in Fig. 9 are similar to those displayed in Fig. 8 for the case of a single mode sine profile for the small scale shear, except than in Fig. 9 the magnitudes of the ratio max F_e/max U_e is magnified. One noticeable difference is that in Fig. 9 the curves are not monotonic and clearly the maximum value of the ratio max F_e/max U_e occur for finite values of λ. Notice also that as the mean flow intensity increases, the location of the maxima shifts towards higher values in the turbulence intensity λ. For the large values $\bar{\lambda}=5$ and 20, the corresponding maxima is modest, 1.55 and 1.29, respectively. Finally, Fig. 9 shows that max F_e is an order of magnitude larger than max U_e over a wide range in the turbulent intensity λ, provided that the mean flow intensity $\bar{\lambda}$ is close enough to the threshold value of $\bar{\lambda}=2$.

V. CONCLUSIONS

Here we analyzed the averaged G-equation and compared its predictions with those obtained from the complete nonlinear averaging theory[12,13] for special flow fields (2) involving a constant mean plus a small-scale shear fluctuation. In this setting, we developed exact formulas for comparing the complete theory with the approximation through averaging the G-equation. We showed that the averaged G-equation theory always underpredicts the flame velocities obtained from the complete averaging theory. When the transverse component of the mean relative to the shear is smaller than one the discrepancies are small with errors typically of a few to roughly 10% in the maximum enhanced flame speed ratio and the agreement in the predicted flame speeds is excellent. On the other hand, when the transverse mean component is larger than one the differences between the predictions of both theories can be very substantial. For values of the transverse mean exceeding one the predictions of both theories can easily differ by an order of magnitude over a large range of turbulent intensities. It is very interesting to develop further comparisons of enhanced flame speeds between the complete nonlinear averaging theory summarized in Sec. II and the averaged G-equation from Sec. III for more realistic periodic flow fields such as arrays of vortices.

ACKNOWLEDGMENTS

P. F. Embid research is partially supported by DARPA under Grant No. N00014-92-J-1796; A. J. Majda research is partially supported by ARO under Grant No. DAAL03-92-G-0010, by DARPA under Grant No. N00014-92-J-1796, by ONR under Grant No. N00014-89-J-1044.P0003, and by NSF under Grant No. DMS-99301094; and P. E. Souganidis research is partially support by NSF under Grant Nos. DMS-9025617 and DMS-9296117 (PYI), by ONR under Grant No. N00014-93-1-0015, by ARO under Grant No. DAAL03-90-G-0012, and by the Alfred P. Sloan Foundation.

[1]R. G. Abdel-Gayed, K. J. Al-Khishali, and D. Bradley, "Turbulent burning velocities and flame straining in explosions," Proc. R. Soc. London Ser. A **391**, 394 (1984).

[2]R. G. Abdel-Gayed, D. Bradley, M. N. Hamid, and M. Lawes, "Lewis number effects on turbulent burning velocity," in *Twentieth Symposium (International) on Combustion* (The Combustion Institute, 1984), pp. 505–512.

[3]W. T. Ashurst and G. I. Sivashinsky, "On flame propagation through periodic flow fields," Combust. Sci. Technol. **80**, 159 (1991).

[4]A. R. Kerstein, W. T. Ashurst, and F. A. Williams, "Field equation for interface propagation in an unsteady homogeneous flow field," Phys. Rev. A **37**, 2728 (1988).
[5]A. R. Kerstein and W. T. Ashurst, "Propagation rate of growing interfaces in stirred fluids," Phys. Rev. Lett. **68**, 934 (1992).
[6]N. Peters, "A spectral closure for premixed turbulent combustion in the flamelet regime," J. Fluid. Mech. **242**, 611 (1992).
[7]G. I. Sivashinsky, "Cascade renormalization theory of turbulent flame speed," Combust. Sci. Technol. **62**, 77 (1988).
[8]V. Yakhot, "Propagation velocity of premixed turbulent flames," Combust. Sci. Technol. **60**, 191 (1988).
[9]P. Clavin and F. A. Williams, "Theory of premixed-flame propagation in large-scale turbulence," J. Fluid Mech. **90**, 589 (1979).
[10]P. Clavin and F. A. Williams, "Effects of molecular diffusion and of thermal expansion on the structure and dynamics of premixed flames in turbulent flows of large and low intensity," J. Fluid Mech. **116**, 251 (1982).
[11]M. Matalon and B. J. Matkowsky, "Flames as gas dynamics discontinuities," J. Fluid Mech. **124**, 239 (1982).
[12]A. J. Majda and P. E. Souganidis, "Large scale front dynamics for turbulent reaction–diffusion equations with separated velocity scales," Nonlinearity **7**, 1 (1994).
[13]P. F. Embid, A. J. Majda, and P. E. Souganidis, "Effective geometric front dynamics for premixed turbulent combustion with separated velocity scales," Combust. Sci. Technol. **103**, 85 (1994).
[14]Y. B. Zeldovich, G. I. Barenblatt, V. B. Librovich, and G. M. Makhviladze, *The Mathematical Theory of Combustion and Explosions* (Consultants Bureau, New York, 1985).
[15]P. L. Lions, G. Papanicolaou, and S. R. S. Varadhan, "Homogenization of Hamilton–Jacobi equations," preprint.
[16]L. C. Evans, "Periodic homogeneization of certain fully nonlinear partial differential equations," Proc. R. Soc. Edinburgh **120A**, 245 (1992).